

# Gradient Flow of Energy: A General and Efficient Approach for Entity Alignment Decoding

Yuanyi Wang

State Key Laboratory of Networking  
and Switching Technology, Beijing  
University of Posts and  
Telecommunications  
Beijing, China  
wangyuanyi@bupt.edu.cn

Haifeng Sun

State Key Laboratory of Networking  
and Switching Technology, Beijing  
University of Posts and  
Telecommunications  
Beijing, China  
hfsun@bupt.edu.cn

Jingyu Wang

State Key Laboratory of Networking  
and Switching Technology, Beijing  
University of Posts and  
Telecommunications  
Beijing, China  
wangjingyu@bupt.edu.cn

Qi Qi

State Key Laboratory of Networking  
and Switching Technology, Beijing  
University of Posts and  
Telecommunications  
Beijing, China  
qiqi8266@bupt.edu.cn

Shaoling Sun

China Mobile (Suzhou) Software  
Technology Co., Ltd.  
Jiangsu, China  
sunshaoling@cmss.chinamobile.com

Jianxin Liao

State Key Laboratory of Networking  
and Switching Technology, Beijing  
University of Posts and  
Telecommunications  
Beijing, China  
jxlbt@bupt.edu.cn

## ABSTRACT

Entity alignment (EA), a pivotal process in integrating multi-source Knowledge Graphs (KGs), seeks to identify equivalent entity pairs across these graphs. Most existing approaches regard EA as a graph representation learning task, concentrating on enhancing graph encoders. However, the decoding process in EA - essential for effective operation and alignment accuracy - has received limited attention and remains tailored to specific datasets and model architectures, necessitating both entity and additional explicit relation embeddings. This specificity limits its applicability, particularly in GNN-based models. To address this gap, we introduce a novel, generalized, and efficient decoding approach for EA, relying solely on entity embeddings. Our method optimizes the decoding process by minimizing Dirichlet energy, leading to the gradient flow within the graph, to promote graph homophily. The discretization of the gradient flow produces a fast and scalable approach, termed Triple Feature Propagation (TFP). TFP innovatively channels gradient flow through three views: *entity-to-entity*, *entity-to-relation*, and *relation-to-entity*. This generalized gradient flow enables TFP to harness the multi-view structural information of KGs. Rigorous experimentation on diverse real-world datasets demonstrates that our approach significantly enhances various EA methods. Notably, the approach achieves these advancements with less than 6 seconds of additional computational time, establishing a new benchmark in efficiency and adaptability for future EA methods.

## CCS CONCEPTS

• **Computing methodologies** → **Knowledge representation and reasoning**; • **Information systems** → **Information integration**.

## KEYWORDS

Entity Alignment, Knowledge Graphs, Dirichlet Energy, Gradient Flow, Decoder, Triple Feature Propagation

## 1 INTRODUCTION

Knowledge Graphs (KGs) have emerged as crucial tools in diverse fields, including information retrieval [48], question answering [1, 4], recommendation systems [6, 38], and natural language processing [12]. Despite their growing relevance, KGs are hindered by coverage limitations, which diminish their utility in various applications. A core challenge in leveraging heterogeneous KGs lies in Entity Alignment (EA) - the process of identifying analogous entities across different KGs. EA typically unfolds in two phases: encoding and decoding (Fig. 1). Current EA methods heavily rely on seed alignments for supervised learning of entity representations, thereby encoding KGs into a unified embedding space and subsequently decoding these embeddings to deduce alignments.

Historically, EA has been viewed as a graph representation learning task, with a focus on enhancing graph encoders. These encoders are broadly categorized into translation-based and Graph Neural Networks (GNN)-based models. Translation-based encoders, like TransE [3] and its variants [5, 10], interpret relation embeddings as translation vectors from the subject entity embedding to the object entity. Conversely, GNN-based encoders, exemplified by GCN-Align [39], MRAEA [23], and Dual-AMN [20], generate entity representations by aggregating neighboring embeddings, each introducing unique improvements to capture long-term relational dependencies and accelerate training.

Despite these advancements in encoders, research on EA decoders [36] has been limited and tailored to specific datasets and model architectures. The prevalent decoder, *greedy search*, prioritizes the nearest neighbor based on entity embedding similarity. This approach, however, can lead to multiple alignments for a single entity, which violates the inherent one-to-one mapping principle of EA. Approaches like CSLS [14] attempt to normalize the similarity matrix using local nearest neighbors, while recent studies [45, 54] consider global alignment strategies, treating decoding as a one-to-one assignment problem, solvable via algorithms like the

Hungarian [13] or Sinkhorn [8]. Yet, these methods primarily re-purpose existing algorithms without deeply exploring the intrinsic properties of KGs, particularly their structural information. DATTI [19] makes strides in this direction by decoding entity and relation embeddings using Third-order Tensor Isomorphism. However, its applicability is limited as it requires explicit relation embeddings, which many GNN-based encoders do not provide.

In alignment with the principles of graph encoders, we assert that an effective EA decoding approach should fulfill two key criteria: (i) the ability to exploit the structural information inherent in KGs, and (ii) the capacity to generalize across various types of graph encoders. Regarding the first criterion, it is essential to consider both the distribution characteristics of the graph representations generated by the encoders and the intrinsic structural information of the KGs during the decoding phase. For the second criterion, the approach should be adaptable to both translation-based and GNN-based encoder architectures. A notable distinction lies in the fact that translation-based encoders typically produce explicit relation embeddings along with entity embeddings, whereas most GNN-based encoders primarily generate entity embeddings, embedding relational information implicitly. Despite this, some GNN-based encoders do extract explicit relation embeddings based on entity embedding, underscoring that entity embeddings are central to the graph representation.

In this work, we introduce a general and efficient EA decoding approach designed to leverage the structural information of KGs exclusively through entity embeddings. Distinct from recent methods [9, 11], our approach facilitates the gradient flow of Dirichlet energy for information propagation across all graph encoder types, fully harnessing KGs' structural information without necessitating additional information. This approach is a multi-view propagation-based entity embedding reconstruction step, i.e., the decoding process, subsequent to the graph encoding phase. The reconstruction is anchored in the minimization of Dirichlet energy, which initiates gradient flow within the graph to propagate information effectively. This leads to the development of a rapid and scalable approach, which we have termed **Triple Feature Propagation (TFP)**. TFP is predicated on third-order tensor representations [19] and utilizes three-view structural matrices—*entity-to-entity*, *entity-to-relation*, and *relation-to-entity*—to depict KG structures. This approach marks a departure from traditional adjacency matrices that focus solely on entity-to-entity structural information. TFP then innovatively channels gradient flow through these multi-view matrices, offering a novel perspective in KG representation and alignment.

To rigorously assess our proposed method, we applied TFP across both translation-based and GNN-based graph encoders, encompassing four sophisticated EA methods. Our experimental analysis of widely recognized public datasets revealed that TFP achieves remarkable performance enhancements. Specifically, we observed a 31.44% increase in Hits@1 and a 21.38% increase in MRR for translation-based encoders. Impressively, even when applied to the state-of-the-art (SOTA) EA methods, TFP secured a 2.25% improvement in Hits@1. These advancements are achieved with less than 6 seconds of additional computational time, a duration trivial in comparison to the overall training process. This efficiency sets a new precedent in both efficiency and adaptability for future EA methods. Our contributions through this work are multifaceted:

- **Innovative Approach:** We introduce TFP, a general and efficient decoding approach that elevates alignment accuracy by leveraging structural information through entity embeddings alone, compatible across various graph encoder types.
- **Theoretical Analysis:** TFP emerges naturally as the gradient flow that minimizes Dirichlet energy, which can be interpreted as a graph heat equation with aligned embeddings as boundary conditions. We detail the discretization of this gradient flow and present an explicit Euler solution.
- **Extensive Experiments:** Our comprehensive experimentation on public datasets demonstrates that TFP significantly enhances performance, even when applied to state-of-the-art methods, while the extra required time is less than 6 seconds.

The structure of the paper is outlined as follows: Section 2 delves into related work on EA encoders and decoders. Section 3 defines the problem space and introduces related concepts. Section 4 discusses the gradient flow of Dirichlet energy and presents the Triple Feature Propagation methodology. Experimental outcomes are presented in Section 5, and the paper culminates with conclusions in Section 6.

## 2 RELATED WORK

**Entity Alignment Encoders.** EA is commonly conceptualized as a graph representation learning task. Current EA graph encoders are primarily designed to capture the intricate graph structures of KGs [50]. Broadly, these encoders are categorized into two types: translation-based and Graph Neural Network (GNN)-based. Translation-based EA encoders, which include TransE [3] and its variants [5, 10, 27], focus on embedding learning. In contrast, GNN-based encoders employ various GNN architectures to generate entity embeddings, ranging from vanilla GCNs [39] to more advanced forms like multi-hop GCNs [35], relational GCNs [49], graph attention networks [20, 32, 53], and self-supervised GCNs [15]. Beyond these foundational encoder types, additional enhancements have been explored, including semi-supervised [15, 23] and active learning techniques [2, 16, 51], as well as the incorporation of supplementary information like entity attributes or temporal data [17, 31, 37, 41, 43, 44]. Our Triple Feature Propagation (TFP) strategy, a novel decoding approach, complements these encoders by improving entity representation quality through feature propagation, a process naturally emerging from the gradient flow of Dirichlet Energy. TFP is versatile, enhancing any graph encoder, and compatible with the aforementioned advanced techniques.

**Entity Alignment Decoders.** Traditional EA decoders primarily focus on identifying equivalent entities using the embeddings learned by encoders. The most prevalent of these is the *greedy search* algorithm [30, 47], which calculates pairwise entity similarities and selects the most similar pair as the alignment. However, this method often leads to multiple alignments for a single entity, violating EA's one-to-one constraint. To address this, the Cross-Domain Similarity Local Scaling (CSLS) [14] normalizes the similarity matrix using local nearest neighbors, enhancing EA performance. Another approach, the deferred acceptance algorithm [29], seeks stable matching between entities, yielding more accurate results than CSLS. Recent studies [45, 54] adopt a global alignment strategy, treating

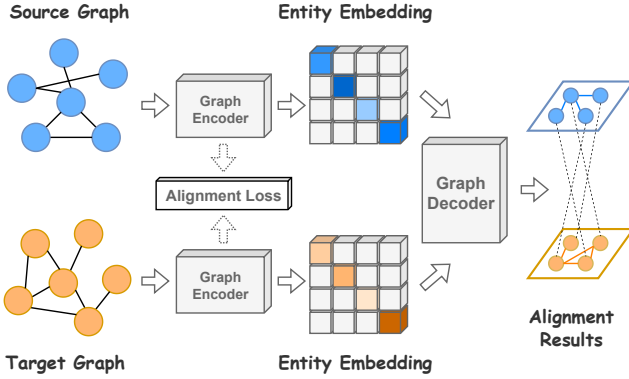


Figure 1: The architecture of existing EA methods.

the decoding process as a one-to-one assignment problem solvable by the Hungarian [13] or Sinkhorn algorithm [8]. However, these methods rely on existing algorithms without sufficiently exploring KGs' unique characteristics, notably their structural information. DATTI [19] represents a step forward, decoding entity and relation embeddings through Third-order Tensor Isomorphism to utilize KG structural information. Despite its effectiveness, DATTI's applicability is constrained as it necessitates explicit relation embeddings, which many graph encoders, particularly GNN-based models, do not generate. In contrast, TFP focuses solely on entity embeddings, a fundamental output of all graph encoder types, thus offering broad applicability. TFP's unique advantage lies in its natural emergence from minimizing Dirichlet energy, providing better interpretability. Crucially, TFP significantly enhances alignment accuracy with only about 6 seconds needed for the reconstruction step, establishing it as a fast and scalable solution.

### 3 PRELIMINARY

In this paper, we define a Knowledge Graph (KG) as  $\mathcal{G} = (\mathcal{E}, \mathcal{R}, \mathcal{T})$ , consisting of a set of entities  $\mathcal{E}$ , a set of relations  $\mathcal{R}$ , and a set of triples  $\mathcal{T} = \{(h, r, t), |h, t \in \mathcal{E}, r \in \mathcal{R}\}$ . Each triple  $(h, r, t)$  denotes an edge from the head entity  $h$  to the tail entity  $t$  under the relation  $r$ . We commence by defining the Entity Alignment (EA) problem and introducing the pertinent concepts utilized in this study.

**Definition 1. Entity Alignment (EA)** is the process of discovering a one-to-one mapping  $\Phi$  between entities from a source KG  $\mathcal{G}_s = (\mathcal{E}_s, \mathcal{R}_s, \mathcal{T}_s)$  to a target KG  $\mathcal{G}_t = (\mathcal{E}_t, \mathcal{R}_t, \mathcal{T}_t)$ . This mapping is informed by seed alignments  $\Phi' \subseteq \Phi$ , where  $\Phi = \{(e_s, e_t), |e_s \in \mathcal{E}_s, e_t \in \mathcal{E}_t, e_s \equiv e_t\}$ , with  $\equiv$  signifying an equivalence relation between entities  $e_s$  and  $e_t$ . The aim is to guide the encoding of entity representations  $\mathbf{X}$  in a unified embedding space for decoding pairwise similarities.

For a simpler graph structure  $G = (V, E)$  with labels  $y = y_i, i \in V$ , where  $V$  represents the set of vertices and  $E$  the set of edges, the concept of graph homophily is crucial. Homophily indicates the likelihood of connected nodes sharing the same label. Formally, we

define the homophily of a graph  $G$  as follows:

$$\mathcal{H}(G) = \mathbb{E}_{i \in V} \left[ \frac{|\{j \in \mathcal{N}_i^{\text{in}} : y_i = y_j\}|}{|\mathcal{N}_i^{\text{in}}|} \right] \quad (1)$$

Here,  $|\{j \in \mathcal{N}_i^{\text{in}} : y_i = y_j\}|$  quantifies the number of neighbors of node  $i$  in  $V$  sharing the same label  $y_i$  [26]. A graph  $G$  is considered homophilic if  $\mathcal{H}(G) \approx 1$  and heterophilic if  $\mathcal{H}(G) \approx 0$ .

**Definition 2. (Laplacian matrix.)** In the context of an undirected graph  $G$  represented by the adjacency matrix  $\mathbf{A}$ , where  $a_{i,j} = 1$  indicates an edge from node  $j$  to node  $i$ , and 0 otherwise, the Laplacian matrix, denoted as  $\Delta$ , is a positive semi-definite matrix defined as  $\Delta = \mathbf{I} - \tilde{\mathbf{A}}$ .

The normalized adjacency matrix is represented by  $\tilde{\mathbf{A}}$ , and the diagonal degree matrices  $\mathbf{D}_{\text{in}}$  and  $\mathbf{D}_{\text{out}}$  are defined as:

$$\mathbf{D}_{\text{in}} = \text{diag}(\sum_j a_{1j}, \dots, \sum_j a_{nj}) \quad (2)$$

$$\mathbf{D}_{\text{out}} = \text{diag}(\sum_i a_{i1}, \dots, \sum_i a_{in}) \quad (3)$$

The concept of Dirichlet energy is often employed to measure the homophily in graph embeddings. We define it as follows:

**Definition 3. (Dirichlet Energy.)** Given the graph node embedding  $\mathbf{X} \in \mathbb{R}^{N \times d}$ , the graph homophily can be measured by the Dirichlet energy of  $\mathbf{X}$ , which is defined by:

$$\mathcal{L}(\mathbf{X}) = \frac{1}{2} \text{tr}(\mathbf{X}^\top \Delta \mathbf{X}) = \frac{1}{4} \sum_{i,j=1}^N a_{i,j} \left\| \frac{\mathbf{X}_i}{\sqrt{\mathbf{D}_{i,i}^{\text{in}} + 1}} - \frac{\mathbf{X}_j}{\sqrt{\mathbf{D}_{j,j}^{\text{out}} + 1}} \right\|^2 \quad (4)$$

## 4 METHODOLOGY

In this section, we introduce our proposed decoding approach, Triple Feature Propagation (TFP). Since the Laplacian matrix  $\Delta$  is derived from the undirected adjacency matrix, which captures the entity-to-entity structure, we initially focus on gradient flow within this special situation before extending the approach to general directed graphs. Our methodology comprises four components: (1) Gradient Flow, (2) Discretization Strategy, (3) Generalized Feature Propagation, and (4) Triple Propagation, grounded on entity embeddings  $\mathbf{X} \in \mathbb{R}^{|\mathcal{E}| \times d}$  produced by a graph encoder.

### 4.1 Gradient Flow

Given seed alignment entity features  $\mathbf{x}_s$ , our objective is to reconstruct the features  $\mathbf{x}_o$  of other entities by minimizing the Dirichlet energy  $\mathcal{L}(\mathbf{X})$ . We designate the set of seed alignment entities as  $\mathcal{E}_s \subseteq \mathcal{E}$ , with the remaining entities denoted by  $\mathcal{E}_o = \mathcal{E} \setminus \mathcal{E}_s$ . The entities are ordered such that:

$$\mathbf{X} = \begin{pmatrix} \mathbf{x}_s \\ \mathbf{x}_o \end{pmatrix}, \quad \Delta = \begin{pmatrix} \Delta_{ss} & \Delta_{so} \\ \Delta_{os} & \Delta_{oo} \end{pmatrix} \quad (5)$$

The gradient flow of Dirichlet energy results in the graph heat equation [7], with seed alignment features remaining stationary. This is expressed as:

$$\frac{d\mathbf{X}(t)}{dt} = -\nabla_{\mathbf{X}} \mathcal{L}(\mathbf{X}(t)) = -\Delta \mathbf{X}(t) \quad (6)$$

By integrating the boundary condition  $\mathbf{x}_s(t) = \mathbf{x}_s$ , the solution to this heat equation provides the required decoding process. The

gradient flow for seed alignments is  $\mathbf{0}$ , leading to the compact expression:

$$\begin{aligned} \frac{d}{dt} \begin{pmatrix} \mathbf{x}_s(t) \\ \mathbf{x}_o(t) \end{pmatrix} &= - \begin{pmatrix} \mathbf{0} & \mathbf{0} \\ \Delta_{os} & \Delta_{oo} \end{pmatrix} \begin{pmatrix} \mathbf{x}_s \\ \mathbf{x}_o(t) \end{pmatrix} \\ &= \begin{pmatrix} \mathbf{0} \\ -\Delta_{os}\mathbf{x}_s - \Delta_{oo}\mathbf{x}_o(t) \end{pmatrix} \end{aligned} \quad (7)$$

Given the positive semi-definite nature of the graph Laplacian matrix, Dirichlet energy  $\mathcal{L}$  is convex, and its global minimizer is the solution to the gradient equation  $\nabla \mathcal{L}(\mathbf{X}(t)) = \mathbf{0}$ . The solution in equation (7) can be expressed as:

$$\frac{d\mathbf{x}_o(t)}{dt} = -\Delta_{os}\mathbf{x}_s - \Delta_{oo}\mathbf{x}_o(t) = \mathbf{0} \quad (8)$$

Therefore, we present the following proposition:

**Proposition 1. (Existence of the solution.)** *The matrix  $\Delta_{oo}$  is non-singular, allowing the reconstruction of other entity features  $\mathbf{x}_o$  using seed alignment entity features  $\mathbf{x}_s$  as  $\mathbf{x}_o(t) = -\Delta_{oo}^{-1}\Delta_{os}\mathbf{x}_s$ .*

PROOF. Initially, consider an undirected connected graph scenario where  $\Delta_{oo}$  is a sub-matrix of the Laplacian matrix  $\Delta$ . Given that sub-Laplacian matrices of undirected connected graphs are invertible [28], thus  $\Delta_{oo}$  is non-singular. The spectral properties of eigenvalues in undirected graphs suggest similar non-singularity for directed graphs [25].

For general cases, assume an ordered representation of the adjacency matrix for a disconnected graph as:

$$\mathbf{A} = \text{diag}(\mathbf{A}_1, \dots, \mathbf{A}_r) \quad (9)$$

Here,  $\mathbf{A}_i, i = 1, \dots, r$ , represents each connected component. The gradient flow in equation (8) is applicable to each connected component independently for disconnected graphs.  $\square$

However, solving this system of linear equations is computationally intensive, with a complexity of  $O(|\mathcal{E}_o|^3)$  for matrix inversion, rendering it impractical for large graphs.

**Remark.** This special gradient flow in TFP is generalized to directed graphs, distinguishing it from FP [28] on undirected graphs.

## 4.2 Discretization Strategy

To tackle the computational challenges, we discretize the heat equation (7) and adopt an iterative numerical approach for its resolution. By approximating the temporal derivative as a forward difference and discretizing time  $t$  with fixed steps ( $t = hk$  for step size  $h > 0$  and  $k = 1, 2, \dots$ ), we employ the implicit Euler scheme:

$$\mathbf{X}^{(k+1)} = \mathbf{X}^{(k)} + h \frac{d\mathbf{X}(t)}{dt} \mathbf{X}^{(k)} \quad (10)$$

Incorporating the heat equation (6), the explicit Euler scheme is subsequently defined as:

$$\mathbf{X}^{(k+1)} = \begin{pmatrix} \mathbf{I} & \mathbf{0} \\ -h\Delta_{os} & \mathbf{I} - h\Delta_{oo} \end{pmatrix} \mathbf{X}^{(k)} \quad (11)$$

When focusing on the special case of  $h = 1$ , we can use the following observation to rewrite the iteration formula.

$$\tilde{\mathbf{A}} = \mathbf{I} - \Delta = \begin{pmatrix} \mathbf{I} - \Delta_{ss} & -\Delta_{so} \\ -\Delta_{os} & \mathbf{I} - \Delta_{oo} \end{pmatrix} \quad (12)$$

$$\mathbf{X}^{(k+1)} = \begin{pmatrix} \mathbf{I} & \mathbf{0} \\ \tilde{\mathbf{A}}_{os} & \tilde{\mathbf{A}}_{oo} \end{pmatrix} \mathbf{X}^{(k)} \quad (13)$$

This Euler scheme serves as a gradient descent for the Dirichlet energy, reducing the energy and smoothing the features. The approximation of this solution in this case is formalized as follows:

**Proposition 2. (Approximation of the solution.)** *With the iterative reconstruction solution as delineated in equation (13), and considering a sufficiently large iteration count  $N$ , the entity features will approximate the results of feature propagation as follows:*

$$\mathbf{X}^{(N)} \approx \begin{pmatrix} \mathbf{x}_s \\ \Delta_{oo}^{-1} \tilde{\mathbf{A}}_{os} \mathbf{x}_s \end{pmatrix} \quad (14)$$

PROOF. Commencing with the initial entity features  $\mathbf{X}^{(0)}$  generated by EA encoders and applying equation (13), we iterate:

$$\begin{aligned} \begin{pmatrix} \mathbf{x}_s^{(k)} \\ \mathbf{x}_o^{(k)} \end{pmatrix} &= \begin{pmatrix} \mathbf{I} & \mathbf{0} \\ \tilde{\mathbf{A}}_{os} & \tilde{\mathbf{A}}_{oo} \end{pmatrix} \begin{pmatrix} \mathbf{x}_s^{(k-1)} \\ \mathbf{x}_o^{(k-1)} \end{pmatrix} \\ &= \begin{pmatrix} \mathbf{x}_s^{(k-1)} \\ \tilde{\mathbf{A}}_{os} \mathbf{x}_s^{(k-1)} + \tilde{\mathbf{A}}_{oo} \mathbf{x}_o^{(k-1)} \end{pmatrix} \end{aligned} \quad (15)$$

Given the stationary nature of the seed alignment entity features  $\mathbf{x}_s$ , we have the equation  $\mathbf{x}_s^{(k)} = \mathbf{x}_s^{(k-1)} = \mathbf{x}_s$ . The focus then shifts to the convergence of  $\mathbf{x}_o^{(k)}$ :

$$\mathbf{x}_o^{(k)} = \tilde{\mathbf{A}}_{os} \mathbf{x}_s + \tilde{\mathbf{A}}_{oo} \mathbf{x}_o^{(k-1)} \quad (16)$$

Expanding and analyzing the limit for the stationary state, we find:

$$\begin{aligned} \lim_{k \rightarrow \infty} \mathbf{x}_o^{(k)} &= \tilde{\mathbf{A}}_{os} \mathbf{x}_s + \lim_{k \rightarrow \infty} \sum_{i=2}^k \tilde{\mathbf{A}}_{oo}^{i-1} \tilde{\mathbf{A}}_{os} \mathbf{x}_s + \lim_{k \rightarrow \infty} \tilde{\mathbf{A}}_{oo}^n \mathbf{x}_o^{(0)} \\ &= \lim_{k \rightarrow \infty} \tilde{\mathbf{A}}_{oo}^n \mathbf{x}_o^{(0)} + \lim_{k \rightarrow \infty} \sum_{i=1}^k \tilde{\mathbf{A}}_{oo}^{i-1} \tilde{\mathbf{A}}_{os} \mathbf{x}_s \end{aligned} \quad (17)$$

Spectral graph theory provides critical insights into the properties of the Laplacian matrix  $\Delta$ . It establishes that the eigenvalues of  $\Delta$  are confined within the range  $[0, 2]$ . This spectral characteristic has direct implications for the matrix  $\tilde{\mathbf{A}} = \mathbf{I} - \Delta$ , whose eigenvalues are consequently within the range  $(-1, 1]$ . A pivotal aspect of this discussion, as elucidated in Proposition 1, is the non-singularity of  $\Delta_{oo}$ . The absence of 0 as an eigenvalue of  $\Delta_{oo}$  implies that  $\tilde{\mathbf{A}}$ 's eigenvalues strictly occupy the interval  $(-1, 1)$ , thereby excluding the endpoints. This spectral behavior significantly influences the convergence properties of the iterative process. Specifically, the limit  $\lim_{k \rightarrow \infty} \tilde{\mathbf{A}}_{oo}^n \mathbf{x}_o^{(0)}$  approaches 0. Furthermore, the summation  $\lim_{k \rightarrow \infty} \sum_{i=1}^k \tilde{\mathbf{A}}_{oo}^{i-1}$  converges to  $(\mathbf{I} - \tilde{\mathbf{A}})^{-1} = \Delta_{oo}^{-1}$ . By integrating these insights, the long-term behavior of the iterative solution can be articulated as:

$$\lim_{k \rightarrow \infty} \mathbf{x}_o^{(k)} = \Delta_{oo}^{-1} \tilde{\mathbf{A}}_{os} \mathbf{x}_s \quad (18)$$

Therefore, when the number of iterations  $N$  is sufficiently large, the entity features in  $\mathbf{x}_o^{(N)}$  approximate  $\Delta_{oo}^{-1} \tilde{\mathbf{A}}_{os} \mathbf{x}_s$ .  $\square$

The update process in Equation (13) equates to initially multiplying the entity features  $\mathbf{X}$  by the matrix  $\tilde{\mathbf{A}}$ , followed by resetting the seed alignment features to their original values. This results in

a highly scalable and straightforward strategy for reconstructing other entity features:

$$\mathbf{X}^{(k+1)} \leftarrow \tilde{\mathbf{A}}\mathbf{X}^{(k)}; \quad \mathbf{x}_s^{(k+1)} \leftarrow \mathbf{x}_s^{(k)} \quad (19)$$

### 4.3 Generalized Feature Propagation

Our discussion has thus far established that the gradient flow of Dirichlet energy facilitates feature reconstruction within basic graph structures. However, KGs extend beyond the realm of simple directed graphs represented by an adjacency matrix  $\mathbf{A}$ . KGs encompass a richer structure, with triples  $\mathcal{T} = \{(h, r, t), |h, t \in \mathcal{E}, r \in \mathcal{R}\}$ , highlighting three distinct structural perspectives: entity-to-entity ( $h - t$ ), entity-to-relation ( $h - r$ ), and relation-to-entity ( $r - t$ ). These perspectives encapsulate key meta-structures in KGs:

- (1) **Entity-to-Relation.** Beyond the conventional adjacency matrix, the  $(h, r)$  pairs in triples provide a unique structural perspective, indicating directional links from head entity  $h$  to relation  $r$ . This directionality is fundamental and unidirectional. For instance, in the triple  $(\text{London}, \text{CapitalOf}, \text{English})$ , the node  $[\text{English}]$  is connected to  $[\text{London}]$  via the relation  $[\text{CapitalOf}]$ , but not in reverse. Similar to the adjacency matrix  $\mathbf{A}$ , we define an *entity to relation* matrix  $\mathbf{A}^{\text{proximal}} \in \mathbb{R}^{|\mathcal{E}| \times |\mathcal{R}|}$  based on the  $(h, r)$  pairs as:

$$\begin{aligned} \mathbf{A}_{i,j}^{\text{proximal}} &= 1, (h_i, r_j) \in \mathcal{T} \\ \mathbf{A}_{i,j}^{\text{proximal}} &= 0, (h_i, r_j) \notin \mathcal{T} \end{aligned} \quad (20)$$

- (2) **Relation-to-Entity.** This category, akin to *entity to relation*, encompasses directed and irreversible information. It underscores the more distant positional relationships between relations and tail entities. The resulting structural matrix,  $\mathbf{A}^{\text{distal}} \in \mathbb{R}^{|\mathcal{R}| \times |\mathcal{E}|}$ , is defined as:

$$\begin{aligned} \mathbf{A}_{i,j}^{\text{distal}} &= 1, (r_i, t_j) \in \mathcal{T} \\ \mathbf{A}_{i,j}^{\text{distal}} &= 0, (r_i, t_j) \notin \mathcal{T} \end{aligned} \quad (21)$$

- (3) **Entity-to-Entity.** Representing the fundamental structural category, this is similar to the adjacency matrix  $\mathbf{A}$ . While  $\mathbf{A}$  provides a solid foundation and is rich in spectral properties, it is insufficient to fully represent KG structures. For example, the triples  $(\text{London}, \text{CapitalOf}, \text{English})$  are structurally distinct with  $(\text{London}, \text{LocateIn}, \text{English})$  in KGs, yet a traditional adjacency matrix treats them identically as they both represent *London* connects *English*. To better represent these nuances, we extend the adjacency matrix to  $\mathbf{A}^{\text{integral}} \in \mathbb{R}^{|\mathcal{E}| \times |\mathcal{E}|}$ :

$$\begin{aligned} \mathbf{A}_{i,i}^{\text{integral}} &= |\mathcal{T}_{e_i}|, e_i \in \mathcal{E} \\ \mathbf{A}_{i,j}^{\text{integral}} &= |\mathcal{T}_{(h_i, t_j)}|, (h_i, t_j) \in \mathcal{T} \end{aligned} \quad (22)$$

$|\mathcal{T}_{e_i}|$  denotes the number of triples involving entity  $e_i$ , and  $|\mathcal{T}_{(h_i, t_j)}|$  indicates the count of triples with the pair  $(h_i, t_j)$ .

Importantly,  $\mathbf{A}_{i,j}^{\text{integral}}$  also preserves the directional characteristics of the KG.

Having established that the gradient flow of Dirichlet energy facilitates reconstruction based on common adjacency relationships

as outlined in equation (13), we extend this concept to the specialized adjacency matrices of KGs. We posit that  $\mathbf{A}^{\text{proximal}}$ ,  $\mathbf{A}^{\text{distal}}$ , and  $\mathbf{A}^{\text{integral}}$ , representing different facets of KG structure, possess analogous spectral properties. Consequently, the gradient flow should yield comparable solutions across these matrices. Specifically,  $\mathbf{A}^{\text{proximal}}$ ,  $\mathbf{A}^{\text{distal}}$ , and  $\mathbf{A}^{\text{integral}}$  encapsulate the adjacency relationships from the head entity to the relation, the relation to the tail entity, and the head entity to the tail entity, respectively.

Utilizing the gradient flow of Dirichlet energy on these three categories of KG structure, we derive a natural and straightforward generalized propagation strategy. The propagation process is articulated through the following equations:

$$\mathbf{X}_r^{(k)} = \mathbf{A}^{\text{distal}} \mathbf{X}_e^{(k)} \quad (23)$$

$$\mathbf{X}_e^{(k+1)} = \mathbf{A}^{\text{integral}} \mathbf{X}_e^{(k)} + \mathbf{A}^{\text{proximal}} \mathbf{X}_r^{(k)} \quad (24)$$

$$\mathbf{x}_s^{(k+1)} = \mathbf{x}_s^{(k)} \quad (25)$$

Here,  $\mathbf{X}_e$  denotes the entity features, initially derived from the graph encoder as  $\mathbf{X}_e^{(0)}$ .  $\mathbf{X}_r$  represents the implicit relation features generated through the propagation strategy. Ultimately, for each entity, the concatenation of entity features from all time steps forms the final outputs:

$$\mathbf{X}_e = [\mathbf{X}^{(0)} || \mathbf{X}^{(1)} || \dots || \mathbf{X}^{(k)}] \quad (26)$$

Crucially, this strategy is solely anchored in the entity embedding  $\mathbf{X}_e^{(0)}$ , a consistent feature across all types of graph encoders.

### 4.4 Triple Propagation

In this subsection, our approach extends beyond capturing and utilizing structural information from three distinct perspectives. Notably, it involves a strategic transfer of features within triples. This process effectively renders the implicit relation feature  $\mathbf{X}_r$  explicit, functioning as a crucial intermediary component. The unique role of relation  $r$  within triple  $\mathcal{E}$  motivates the extension of the relation feature to the triple level via our generalized feature propagation method. We introduce the **triple-to-relation** adjacency matrix  $\mathbf{A}^{\text{tri-rel}} \in \mathbb{R}^{|\mathcal{T}| \times |\mathcal{R}|}$ , defined as:

$$\begin{aligned} \mathbf{A}_{i,j}^{\text{tri-rel}} &= 1, r_j \in \mathcal{T}_i \\ \mathbf{A}_{i,j}^{\text{tri-rel}} &= 0, r_j \notin \mathcal{T}_i \end{aligned} \quad (27)$$

This matrix delineates the connections between triples and relations. To scale and orthogonally project the relation feature  $\mathbf{X}_r$  into a lower  $d_r$  dimensional space, we employ a hyper-sphere independent random projection technique, as suggested by [22].

$$\mathbf{X}_r = \text{ranp}(\mathbf{X}_r) \in \mathbb{R}^{|\mathcal{T}| \times d_r} \quad (28)$$

Consequently, the triple feature  $\mathbf{X}_t$  is generated through:

$$\mathbf{X}_t = \mathbf{A}^{\text{tri-rel}} \mathbf{X}_r \quad (29)$$

Our method enables the representation of the KG structure as a three-dimensional tensor  $\mathbf{A}^{\text{triple}} \in \mathbb{R}^{|\mathcal{E}| \times |\mathcal{E}| \times d_r}$ , rather than the traditional adjacency matrix. The tensor is defined as:

$$\begin{aligned} \mathbf{A}_{h,t}^{\text{triple}} &= \mathbf{X}_t(h, r, t), (h, t) \in \mathcal{T} \\ \mathbf{A}_{h,t}^{\text{triple}} &= 0, (h, t) \notin \mathcal{T} \end{aligned} \quad (30)$$

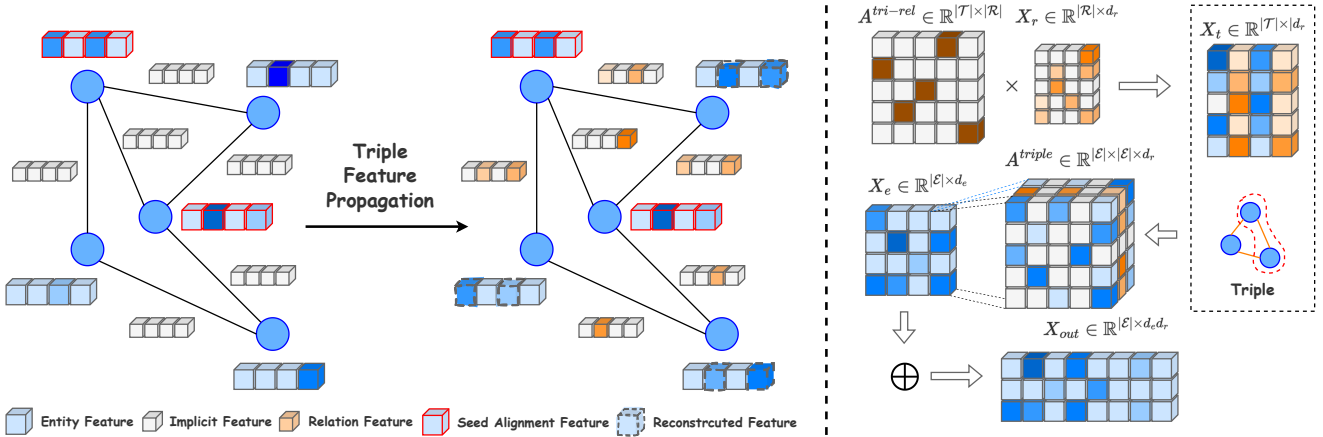


Figure 2: The illustration of Triple Feature Propagation and the process of Triple Propagation.

Here,  $X_t(h, r, t)$  represents the feature of triple  $(h, r, t)$  in  $X_t$ . The KG structure is encapsulated in  $d_r$  slices as  $A_1^{triple}, \dots, A_{d_r}^{triple} \in \mathbb{R}^{|E| \times |E|}$ . Parallel to the relation feature, the entity feature  $X_e$  is also scaled through hyper-sphere independent random projection to  $d_e$  dimension. The propagation process is based on the final entity features  $X_e$ , allowing for the continuation of gradient flow from the triple perspective. Finally, all features are concatenated as follows:

$$X_i = A_i^{triple} X_e, i = 1, \dots, d_r \quad (31)$$

$$X_{out} = [X_1 || X_2 || \dots || X_{d_r}] \quad (32)$$

Our Triple Feature Propagation (TFP) method, stemming from the gradient flow of Dirichlet energy across different structural perspectives, ensures both comprehensive propagation and compatibility with various encoder architectures.

## 5 EXPERIMENTS

In our experimental section, we aim to rigorously evaluate the proposed TFP method. Our key research questions are:

- Q1. Does TFP demonstrate effectiveness and generalizability across various graph encoders? How well does TFP integrate with state-of-the-art (SOTA) methods?
- Q2. How does TFP's performance evolve across iterations when applied to different encoders on various datasets?
- Q3. How does TFP's time efficiency compare to that of encoders?
- Q4. How does TFP perform when additional information is integrated, compared to other textual EA methods?

Our code and data are provided in the anonymous link and will be publicly available upon acceptance.

### 5.1 Experimental Settings

Our experimental setup includes details on datasets, baselines, evaluation metrics, and implementation details.

**5.1.1 Datasets.** We list the statistics of all datasets used in the experiments in Table. 1. We utilize two widely recognized public datasets to test our decoding algorithm: (1) DBP15K [31] comprises

Table 1: Statistics for datasets.

Datasets		Entity	Relation	Triple
DBP <sub>ZH-EN</sub>	Chinese	19388	1701	70414
	English	19572	1323	95142
DBP <sub>JA-EN</sub>	Japanese	19814	1299	77214
	English	19780	1153	93484
DBP <sub>FR-EN</sub>	French	19661	903	105998
	English	19993	1208	115722
SRPRS <sub>FR-EN</sub>	French	15000	177	33532
	English	15000	221	36508
SRPRS <sub>DE-EN</sub>	German	15000	120	37377
	English	15000	222	38363

three cross-lingual subsets from multilingual DBpedia. Each subset contains 15,000 entity pairs. (2) SRPRS [10]. Similar to DBP15K in terms of the number of entity pairs but with fewer triples. For consistency with prior research [5, 39], we use a 30/70 split of pre-aligned entity pairs for training and testing encoders, respectively. Results are averaged over five independent runs.

**5.1.2 Baseline.** To evaluate universality, we evaluate TFP against six advanced EA methods with diverse graph encoders:

- MRAEA [23] is the first method which incorporates meta semantics in relations using GNN-based approach.
- RREA [24] is a GNN-based unified framework enhancing relational representation in triples.
- Dual-AMN [20] is the SOTA of GNN-based methods employing proxy matching and hard negative sampling.
- AlignE [33] is a translation-based method focusing on alignment task optimization through its loss function and negative sampling approach.
- RSN [10] is the sole RNN-based EA encoder, adept at capturing long-term relational dependencies.

- TransEdge [34] is the best translation-based encoder contextualizing relations as edge embeddings.

In addition to the models mentioned above, we are also curious about introducing additional textual information (e.g., entity name) like other studies to provide a multi-aspect view. The methods we compared have been listed in Table.4.

**5.1.3 Evaluation Metrics.** We utilize cosine similarity to calculate the similarity between two entities and employ H@k and MRR as metrics to evaluate all the methods. H@k describes the fraction of truly aligned target entities that appear in the first  $k$  entities of the sorted rank list:

$$H@k = \frac{1}{|S_t|} \sum_{i=1}^{|S_t|} \mathbb{I}[\text{rank}_i \leq k] \quad (33)$$

where  $\text{rank}_i$  refers to the rank position of the first correct mapping for the  $i$ -th query entities and  $\mathbb{I} = 1$  if  $\text{rank}_i \leq k$  and 0 otherwise.  $S_t$  refers to the testing alignment set. MRR (Mean Reciprocal Ranking) is a statistical measure for evaluating many algorithms that produce a list of possible responses to a sample of queries, ordered by the probability of correctness. In the field of EA, the reciprocal rank of a query entity (i.e., an entity from the source KG) response is the multiplicative inverse of the rank of the first correct alignment entity in the target KG. MRR is the average of the reciprocal ranks of results for a sample of candidate alignment entities:

$$MRR = \frac{1}{|S_t|} \sum_{i=1}^{|S_t|} \frac{1}{\text{rank}_i} \quad (34)$$

**5.1.4 Implementaion Details.** The output dimensions  $d$  and other hyper-parameters of all encoders adhere to their original settings in their papers: Dual-AMN ( $d = 768$ ), RREA( $d = 600$ ), MRAEA ( $d = 600$ ), AlignE ( $d = 75$ ), RSN ( $d = 256$ ), and TransEdge ( $d = 75$ ). The iteration  $k$  is set to their best results, which details described in section 3. Other hyper-parameters remain the same for all datasets and methods: relation scale dimension  $d_r = 512$ , entity scale dimension  $d_e = 16$ . All experiments are conducted on a PC with an NVIDIA RTX A6000 GPU and an Intel Xeon Gold 6248R CPU. The code and datasets are submitted through the anonymous link and will be publicly available upon acceptance.

## 5.2 Main Results (Q1)

The core experimental outcomes are summarized in Table 2. Among the evaluated six representative EA methods, Dual-AMN demonstrates superior performance across all datasets, underscoring the efficacy of GNN encoders. Interestingly, TransEdge shows notable success on the DBP15K dataset but underperforms on SRPRS. This can be attributed to TransEdge’s reliance on existing edge semantic information for entity dependency capture, a feature less prevalent in the sparser KGs like SRPRS. Conversely, GNN-based models exhibit robust performance on sparse graphs, highlighting their aptitude for handling sparse topologies.

**5.2.1 GNN-based encoders.** Our TFP method consistently outperforms across all datasets, significantly boosting the performance of all GNN-based baselines. Remarkably, TFP enhances the state-of-the-art Dual-AMN method, achieving performance gains of 2.25% in Hits@1 and 2.02% in MRR on DBP15K<sub>FR-EN</sub>, and 1.28% in Hits@1

and 1.19% in MRR on SRPRS<sub>FR-EN</sub>. These results validate three key points: (i) the gradient flow of Dirichlet energy effectively reconstructs entity embeddings, facilitating feature propagation and preserving homophily; (ii) TFP’s effectiveness and generality across various GNN-based graph encoders; (iii) TFP’s utility and simplicity in augmenting state-of-the-art methods.

**5.2.2 Translation-based encoders.** TFP significantly boosts the performance of translation-based EA encoders, effectively capturing three-view structural information through the gradient flow. Notably, TFP improves AlignE’s performance by 28.87% in Hits@1 on the DBP15K<sub>JA-EN</sub> dataset and by 25.8% on the SRPRS<sub>DE-EN</sub> dataset. For the best translation-based encoder, TransEdge, TFP still achieves substantial enhancements, including at least a 7.01% increase in Hits@1 on DBP15K and 15.22% on SRPRS. These findings demonstrate TFP’s effectiveness and general applicability to translation-based encoders. Particularly, TFP’s significant improvement on the SRPRS dataset indicates its capability to bridge gaps in sparse KG topology understanding, an area where translation-based EA encoders typically struggle.

## 5.3 Exploratory Analysis (Q2)

In this subsection, we delve into the iterative performance of TFP when applied using Dual-AMN and TransEdge encoders on the DBP15K dataset. The results, depicting TFP’s behavior across different iteration counts  $k$ , are illustrated in Figure 3.

**5.3.1 Performance with Dual-AMN Encoder .** Dual-AMN, noted for its exemplary performance in both Hit@k and MRR across DBP15K, provides an insightful context for assessing TFP’s iteration-dependent dynamics. We observe a pattern of stable metric rates on both DBP<sub>ZH-EN</sub> and DBP<sub>JA-EN</sub> subsets. Typically, each evaluation metric displays an initial increase with the iteration count, reaching a plateau or peak, followed by a potential decline due to over-smoothing. For instance, on DBP<sub>ZH-EN</sub>, TFP peaks around  $k = 11$  iterations, beyond which performance stabilizes. However, the Hit@10 metric initially declines before stabilizing, indicating a convergence of the reconstructed features despite random fluctuations. Notably, TFP achieves rapid convergence and significant performance improvements on DBP<sub>FR-EN</sub>, a subset characterized by more comprehensive topological structures due to its construction methodology [31]. Time analysis reveals a proportional increase in computational time with the number of iterations; however, the overall time demand of TFP remains minimal. For instance, even at  $k = 15$  iterations, the processing time remains under 10 seconds, a negligible factor compared to the training duration of the encoder.

**5.3.2 Analysis with TransEdge Encoder.** TransEdge, a leading translation-based encoder, requires fewer iterations for TFP to converge and exhibit significant enhancements. Unlike Dual-AMN, TransEdge excels in capturing higher-level semantic information but falls short in detailing topological structures, a common trait among translation-based encoders. TFP effectively compensates for this limitation by reconstructing entity features that assimilate topological information from three distinct perspectives, thereby enriching the quality of entity features. This implies that during the encoding stage, structural noise due to model bias is minimal, reducing the need for extensive denoising during decoding. Interestingly,

**Table 2: Main experimental results on DBP15K and SRPRS.**

Datasets		DBP <sub>FR-EN</sub>			DBP <sub>JA-EN</sub>			DBP <sub>ZH-EN</sub>			SRPRS <sub>FR-EN</sub>			SRPRS <sub>DE-EN</sub>		
Model		H@1	H@10	MRR	H@1	H@10	MRR	H@1	H@10	MRR	H@1	H@10	MRR	H@1	H@10	MRR
GNN-based	MRAEA	71.63	94.28	80.02	68.7	93.19	77.66	68.7	92.94	77.43	43.44	75.1	53.85	56.18	51.47	64.87
	+TFP	75.45	95.87	83.04	74.26	94.98	82.08	74.4	94.54	81.82	46.06	75.55	55.89	58.83	81.89	66.78
	<b>Improv.</b>	<b>5.33%</b>	<b>1.69%</b>	<b>3.77%</b>	<b>8.09%</b>	<b>1.92%</b>	<b>5.69%</b>	<b>8.30%</b>	<b>1.72%</b>	<b>5.67%</b>	<b>6.03%</b>	<b>0.60%</b>	<b>3.79%</b>	<b>4.72%</b>	<b>59.10%</b>	<b>2.94%</b>
	RREA	73.4	94.8	81.36	70.59	94.13	79.11	70.73	93.21	78.97	42.96	73.96	53.41	56.74	81.24	65.18
	+TFP	80.79	96.98	86.79	78.83	96.0	85.23	79.43	95.45	85.35	47.23	75.6	56.67	59.98	82.33	67.8
	<b>Improv.</b>	<b>10.07%</b>	<b>2.30%</b>	<b>6.67%</b>	<b>11.67%</b>	<b>1.99%</b>	<b>7.74%</b>	<b>12.30%</b>	<b>2.40%</b>	<b>8.08%</b>	<b>9.94%</b>	<b>2.22%</b>	<b>6.10%</b>	<b>5.71%</b>	<b>1.34%</b>	<b>4.02%</b>
	DualAMN	83.43	96.19	88.14	80.31	94.69	85.57	80.39	93.68	85.29	48.28	75.51	57.34	61.2	81.91	68.3
	+TFP	85.31	97.26	89.92	81.26	95.85	86.82	81.64	95.24	86.84	48.9	76.28	58.02	61.84	82.61	69.01
	<b>Improv.</b>	<b>2.25%</b>	<b>1.11%</b>	<b>2.02%</b>	<b>1.18%</b>	<b>1.23%</b>	<b>1.46%</b>	<b>1.55%</b>	<b>1.67%</b>	<b>1.82%</b>	<b>1.28%</b>	<b>1.02%</b>	<b>1.19%</b>	<b>1.05%</b>	<b>0.85%</b>	<b>1.04%</b>
Translation-based	AlignE	53.36	86.55	64.93	50.12	83.91	61.58	50.96	82.3	61.7	34.33	65.44	44.68	44.07	69.43	52.7
	+TFP	68.45	91.96	76.81	64.59	90.77	73.76	66.98	89.78	74.89	42.11	71.8	51.98	55.44	78.61	63.48
	<b>Improv.</b>	<b>28.28%</b>	<b>6.25%</b>	<b>18.30%</b>	<b>28.87%</b>	<b>8.18%</b>	<b>19.78%</b>	<b>31.44%</b>	<b>9.09%</b>	<b>21.38%</b>	<b>22.66%</b>	<b>9.72%</b>	<b>16.34%</b>	<b>25.80%</b>	<b>13.22%</b>	<b>20.46%</b>
	RSN	63.17	86.37	71.33	59.13	81.5	67.03	60.67	82.86	68.53	35.1	63.78	44.73	51.07	74.43	59.02
	+TFP	77.79	92.45	83.73	73.53	91.97	80.04	75.44	91.71	81.33	44.32	73.22	53.97	59.27	81.14	66.84
	<b>Improv.</b>	<b>23.14%</b>	<b>7.04%</b>	<b>17.38%</b>	<b>24.35%</b>	<b>12.85%</b>	<b>19.41%</b>	<b>24.34%</b>	<b>10.68%</b>	<b>18.68%</b>	<b>26.27%</b>	<b>14.80%</b>	<b>20.66%</b>	<b>16.06%</b>	<b>9.02%</b>	<b>13.25%</b>
	TransEdge	76.9	93.97	83.03	74.66	92.93	81.1	76.19	92.16	81.81	40.81	67.66	49.73	55.65	75.3	64.28
	+TFP	82.36	96.9	87.91	80.52	95.96	86.19	81.53	95.21	86.5	49.03	75.22	56.49	64.12	81.7	70.95
	<b>Improv.</b>	<b>7.10%</b>	<b>3.12%</b>	<b>5.88%</b>	<b>7.85%</b>	<b>3.26%</b>	<b>6.28%</b>	<b>7.01%</b>	<b>3.31%</b>	<b>5.73%</b>	<b>20.14%</b>	<b>11.17%</b>	<b>13.59%</b>	<b>15.22%</b>	<b>8.50%</b>	<b>10.38%</b>

Remark: **bold** means the best performance; "Improv." represents the percentage increase of TFP compared with EA encoder results.

**Table 3: Time costs (seconds) of existing EA methods with TFP on DBP15K and SRPRS.**

Translation-based			GNN-based		
Time/s	DBP15K	SRPRS	Time/s	DBP15K	SRPRS
AlignE	2087	1190	MRAEA	1743	558
TFP(CPU)	13.9	8.1	TFP(CPU)	16.6	10.6
TFP(GPU)	4.8	4.2	TFP(GPU)	5.9	4.6
RSN	3659	1279	RREA	323	276
TFP(CPU)	14.2	9.2	TFP(CPU)	16.3	11
TFP(GPU)	4.8	3.7	TFP(GPU)	5.7	3.8
TransEdge	1625	907	DualAMN	177	163
TFP(CPU)	12.9	8.7	TFP(CPU)	17.7	11.4
TFP(GPU)	4.7	3.6	TFP(GPU)	5.1	4.6

an inverse proportionality emerges between iteration count and time cost beyond  $k = 2$ , characterized by a diminishing time requirement with increasing iterations. Our comprehensive experimental analysis attributes this phenomenon to TFP's enhancement of homophily in relational features during the decoding phase leading to over-smoothing, particularly at higher iteration counts. This augmentation results in sparser features as per equations (23) and (29), culminating in over-smoothing that, in turn, leads to a reduction in computational time due to the increased feature sparsity.

#### 5.4 Time Complexity Analysis (Q3)

In this subsection, we assess the computational efficiency of Triple Feature Propagation. TFP's computational process, which primarily

involves iterative sparse-to-dense matrix multiplications, is executed as a discrete, one-time additional step post-training. As delineated in Section 4.4, TFP propagates features across Knowledge Graphs devoid of any trainable parameters, thereby maintaining a computational complexity of  $O(|\mathcal{T}|d_r + |\mathcal{E}|d_e)$ .

In Table 3, we present a detailed comparison of the time costs associated with the training and decoding phases (TFP) across six EA encoders, utilizing both CPU and GPU, on DBP15K and SRPRS datasets. Notably, the propagation step of TFP constitutes only a minor portion of the overall runtime, with the bulk of the time being allocated to the encoder training process. Remarkably, on a GPU, TFP's execution time peaks at just 5.9 seconds. Even when operating on a CPU, TFP requires a maximum of merely 17.7 seconds. This duration is insignificant when contrasted with even the fastest encoder, Dual-AMN.

A comparative observation reveals that TFP's application is expedited on translation-based encoders relative to GNN-based ones. This acceleration is attributable to the varying entity embedding dimensions discussed in Section 5.1.4. The output dimension for GNN-based encoders, particularly for MRAEA and Dual-AMN, is set at  $d = 600$  and  $d = 768$ , respectively, which is larger than that of the translation-based encoders. This discrepancy in dimensionality directly influences the time efficiency of TFP, as demonstrated by the faster performance on translation-based models.

#### 5.5 Additional Information (Q4)

Within the scope of EA, traditional experiments have largely focused on purely structural-based methods. However, contemporary research [42, 46] has introduced supplementary information (entity

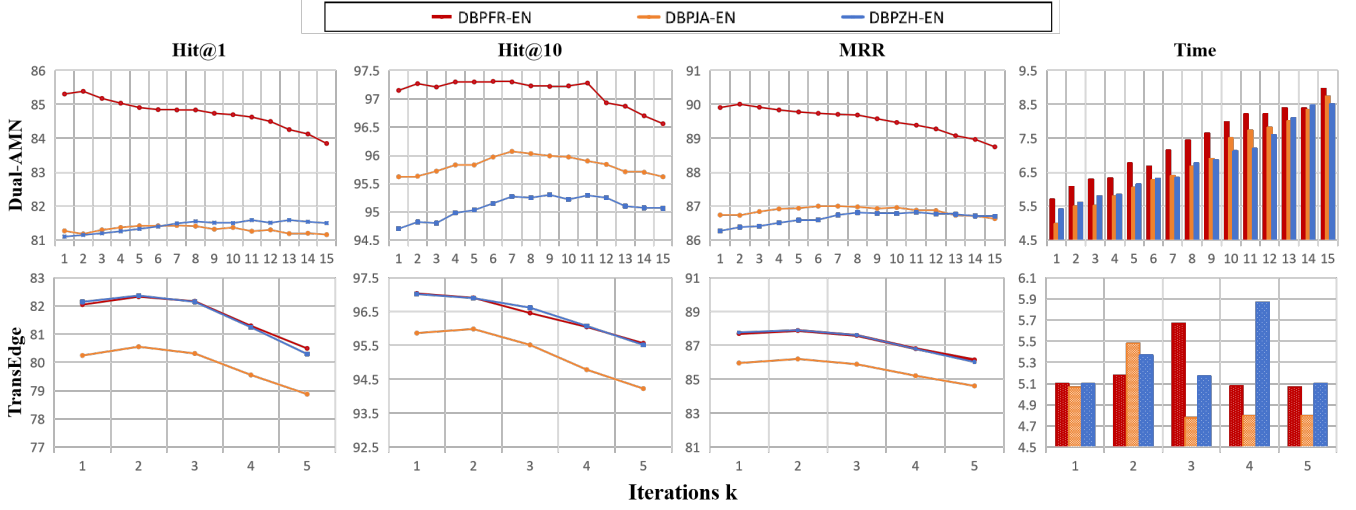
Figure 3: Different evaluation metrics and time cost (second) on DBP15K with different iterations  $k$ .

Table 4: Performances of textual EA methods, which make alignment by additional entity name. The results of baselines are collected from the original papers. TFP(Initial) represents directly using entity name (literal feature) as the initial entity feature and TFP(SEU) represents the initial features generated by SEU.

Datasets	DBP <sub>FR-EN</sub>			DBP <sub>JA-EN</sub>			DBP <sub>ZH-EN</sub>			SRPRS <sub>FR-EN</sub>			SRPRS <sub>DE-EN</sub>		
Models	H@1	H@10	MRR	H@1	H@10	MRR	H@1	H@10	MRR	H@1	H@10	MRR	H@1	H@10	MRR
GM-Align [46]	89.4	95.2	-	73.9	87.2	-	67.9	78.5	-	57.4	64.6	60.2	68.1	74.8	71.0
RDGCN [41]	87.3	95.0	90.1	76.3	89.7	76.3	69.7	84.2	75.0	67.2	76.7	71.0	77.9	88.6	82.0
HGCN [42]	76.6	89.7	81.0	89.2	96.1	91.0	72.0	85.7	76.0	67.0	77.0	71.0	76.3	86.3	80.1
AtrrGNN [18]	91.9	97.9	91.0	78.3	92.0	83.4	79.6	92.9	84.5	-	-	-	-	-	-
EPEA [40]	95.5	98.6	96.7	92.4	96.9	94.2	88.5	95.3	91.1	-	-	-	-	-	-
DAT [52]	-	-	-	-	-	-	-	-	-	75.8	89.9	81.0	87.6	95.5	90.0
SEU [21]	98.8	99.9	99.2	95.6	99.1	96.9	90	96.5	92.4	98.2	99.5	98.6	98.3	99.6	98.7
<b>TFP (Initial)</b>	98.3	99.72	98.87	94.1	97.91	95.49	87.43	94.62	89.98	<b>98.99</b>	<b>99.7</b>	<b>99.28</b>	<b>98.83</b>	<b>99.62</b>	<b>99.12</b>
<b>TFP (SEU)</b>	<b>99.05</b>	<b>99.9</b>	<b>99.4</b>	<b>96.21</b>	<b>98.84</b>	<b>97.19</b>	<b>90.51</b>	<b>96.42</b>	<b>92.63</b>	98.55	99.53	98.95	98.57	99.54	98.95

names) to refine EA performance. These advanced approaches typically employ machine translation systems or cross-lingual word embeddings to transition entity names into a cohesive semantic space, subsequently utilizing averaged pre-trained word embeddings to formulate initial features for both entities and relations. In this enhanced context, initial entity features  $X_e$  are pre-aligned, positioning these textual EA methods akin to decoding algorithms that emphasize topology and dependencies. Consequently, Triple Feature Propagation is capable of fulfilling a similar role, akin to scenarios where seed alignment sets are absent.

To make fair comparisons with these textural-based EA methodologies, we adopted identical entity name translations and pre-trained word embeddings as delineated by Xu et al. [46]. We established two distinct scenarios for this assessment:

- (i) TFP(Initial), which utilizes TFP as a standalone textual EA method on pre-aligned entity name features.
- (ii) TFP(SEU), which employs the textual EA method SEU as the encoder, with TFP acting as the decoder.

Table 4 delineates the performance metrics of TFP(Initial), TFP(SEU), and seven other baseline methods across the DBP15K and SRPRS datasets. Remarkably, TFP, as an unsupervised textual EA method, surpasses all other competitors on DBP15K and secures a near-top placement on SRPRS. Utilizing SEU as an encoder alongside TFP further elevates performance, nearing the benchmark of 100% accuracy. Notably, the comparative results of SEU and TFP exhibit formidable competitiveness, aligning more with propagation strategies than neural network paradigms. This indicates redundancy in current textual EA methodologies, suggesting that the complex neural networks and pre-aligned entity pairs may be unnecessary with pre-aligned initial features.

Despite demonstrating strong competitive prowess, TFP(SEU) exhibits a slight performance decrement compared to the use of initial entity name features exclusively. This can be attributed to the inherent similarities between SEU and TFP: both operate on propagation principles, ostensibly acting as smoothing strategies predicated on topological data assimilation. In scenarios involving sparse KGs,

SEU's ability to comprehensively capture topological nuances and facilitate entity embedding smoothing is significant. However, subsequent application of TFP may precipitate over-smoothing, which elucidates the observed performance discrepancy.

## 6 CONCLUSION

This paper introduces Triple Feature Propagation (TFP), a general and efficient decoding approach for entity alignment. Derived from the gradient flow of Dirichlet energy minimization, TFP implements an iterative process and heat equation matrices, updating features from three unique structural perspectives. It is designed to be universally compatible with all types of EA encoders. Our experiments on real-world datasets demonstrate TFP's ability to significantly enhance performance in advanced EA methods, achieving these improvements with less than 6 seconds of additional computational time. This efficiency and general applicability make TFP a promising advancement in the field of entity alignment.

## REFERENCES

- [1] Farah Atif, Ola El Khatib, and Djellel Difallah. 2023. Beamqa: Multi-hop knowledge graph question answering with sequence-to-sequence prediction and beam search. In *Proceedings of the 46th International ACM SIGIR Conference on Research and Development in Information Retrieval*. 781–790.
- [2] Max Berrendorf, Evgeniy Faerman, and Volker Tresp. 2021. Active learning for entity alignment. In *Advances in Information Retrieval: 43rd European Conference on IR Research, ECIR 2021, Virtual Event, March 28–April 1, 2021, Proceedings, Part I* 43. Springer, 48–62.
- [3] Antoine Bordes, Nicolas Usunier, Alberto Garcia-Duran, Jason Weston, and Oksana Yakhnenko. 2013. Translating embeddings for modeling multi-relational data. *Advances in neural information processing systems* 26 (2013).
- [4] Soumen Chakrabarti. 2022. Deep knowledge graph representation learning for completion, alignment, and question answering. In *Proceedings of the 45th International ACM SIGIR Conference on Research and Development in Information Retrieval*. 3451–3454.
- [5] Muhao Chen, Yingtao Tian, Mohan Yang, and Carlo Zaniolo. 2017. Multilingual knowledge graph embeddings for cross-lingual knowledge alignment. In *Proceedings of the 26th International Joint Conference on Artificial Intelligence*. 1511–1517.
- [6] Qian Chen, Zhiqiang Guo, Jianjun Li, and Guohui Li. 2023. Knowledge-enhanced Multi-View Graph Neural Networks for Session-based Recommendation. In *Proceedings of the 46th International ACM SIGIR Conference on Research and Development in Information Retrieval*. 352–361.
- [7] Fan Chung. 1996. Spectral Graph Theory. In *CBMS Regional Conference Series in Mathematics*. American Mathematical Society.
- [8] Marco Cuturi. 2013. Sinkhorn distances: Lightspeed computation of optimal transport. *Advances in neural information processing systems* 26 (2013).
- [9] Matthias Fey, Jan E Lenssen, Christopher Morris, Jonathan Masci, and Nils M Kriege. 2019. Deep Graph Matching Consensus. In *International Conference on Learning Representations*.
- [10] Lingbing Guo, Zequn Sun, and Wei Hu. 2019. Learning to exploit long-term relational dependencies in knowledge graphs. In *International conference on machine learning*. PMLR, 2505–2514.
- [11] Mark Heimann, Xiyuan Chen, Fatemeh Vahedian, and Danai Koutra. 2021. Refining network alignment to improve matched neighborhood consistency. In *Proceedings of the 2021 SIAM International Conference on Data Mining (SDM)*. SIAM, 172–180.
- [12] Shaoxiong Ji, Shirui Pan, Erik Cambria, Pekka Marttinen, and Philip S. Yu. 2022. A Survey on Knowledge Graphs: Representation, Acquisition, and Applications. *IEEE Trans. Neural Networks Learn. Syst.* 33, 2 (2022), 494–514.
- [13] Harold W Kuhn. 1955. The Hungarian method for the assignment problem. *Naval research logistics quarterly* 2, 1-2 (1955), 83–97.
- [14] Guillaume Lample, Alexis Conneau, Marc'Aurelio Ranzato, Ludovic Denoyer, and Hervé Jégou. 2018. Word translation without parallel data. In *International Conference on Learning Representations*.
- [15] Jia Li and Dandan Song. 2022. Uncertainty-aware pseudo label refinery for entity alignment. In *Proceedings of the ACM Web Conference 2022*. 829–837.
- [16] Bing Liu, Harrison Scells, Guido Zuccon, Wen Hua, and Genhong Zhao. 2021. ActiveEA: Active Learning for Neural Entity Alignment. In *Proceedings of the 2021 Conference on Empirical Methods in Natural Language Processing*. 3364–3374.
- [17] Xiaozhe Liu, Junyang Wu, Tianyi Li, Lu Chen, and Yunjun Gao. 2023. Unsupervised Entity Alignment for Temporal Knowledge Graphs. In *Proceedings of the ACM Web Conference 2023*. 2528–2538.
- [18] Zhiyuan Liu, Yixin Cao, Liangming Pan, Juanzi Li, and Tat-Seng Chua. 2020. Exploring and Evaluating Attributes, Values, and Structures for Entity Alignment. In *Proceedings of the 2020 Conference on Empirical Methods in Natural Language Processing (EMNLP)*. 6355–6364.
- [19] Xinnian Mao, Meirong Ma, Hao Yuan, Jianchao Zhu, Zongyu Wang, Rui Xie, Wei Wu, and Man Lan. 2022. An effective and efficient entity alignment decoding algorithm via third-order tensor isomorphism. In *Proceedings of the 60th Annual Meeting of the Association for Computational Linguistics (Volume 1: Long Papers)*. 5888–5898.
- [20] Xin Mao, Wenting Wang, Yuanbin Wu, and Man Lan. 2021. Boosting the speed of entity alignment 10x: Dual attention matching network with normalized hard sample mining. In *Proceedings of the Web Conference 2021*. 821–832.
- [21] Xinnian Mao, Wenting Wang, Yuanbin Wu, and Man Lan. 2021. From Alignment to Assignment: Frustratingly Simple Unsupervised Entity Alignment. In *Proceedings of the 2021 Conference on Empirical Methods in Natural Language Processing*. 2843–2853.
- [22] Xinnian Mao, Wenting Wang, Yuanbin Wu, and Man Lan. 2022. LightEA: A Scalable, Robust, and Interpretable Entity Alignment Framework via Three-view Label Propagation. In *Proceedings of the 2022 Conference on Empirical Methods in Natural Language Processing*. 825–838.
- [23] Xin Mao, Wenting Wang, Huimin Xu, Man Lan, and Yuanbin Wu. 2020. MRAEA: an efficient and robust entity alignment approach for cross-lingual knowledge graph. In *Proceedings of the 13th International Conference on Web Search and Data Mining*. 420–428.
- [24] Xin Mao, Wenting Wang, Huimin Xu, Yuanbin Wu, and Man Lan. 2020. Relational reflection entity alignment. In *Proceedings of the 29th ACM International Conference on Information & Knowledge Management*. 1095–1104.
- [25] Sohr Maskey, Raffaele Paolino, Aras Bacho, and Gitta Kutyniok. 2023. A Fractional Graph Laplacian Approach to Oversmoothing. *arXiv preprint arXiv:2305.13084* (2023).
- [26] Hongbin Pei, Bingzhe Wei, Kevin Chen-Chuan Chang, Yu Lei, and Bo Yang. 2019. Geom-GCN: Geometric Graph Convolutional Networks. In *International Conference on Learning Representations*.
- [27] Shichao Pei, Lu Yu, Robert Hoehndorf, and Xiangliang Zhang. 2019. Semi-supervised entity alignment via knowledge graph embedding with awareness of degree difference. In *The world wide web conference*. 3130–3136.
- [28] Emanuele Rossi, Henry Kenlay, Maria I Gorinova, Benjamin Paul Chamberlain, Xiaowen Dong, and Michael M Bronstein. 2022. On the unreasonable effectiveness of feature propagation in learning on graphs with missing node features. In *Learning on Graphs Conference*. PMLR, 11–1.
- [29] Alvin E Roth. 2008. Deferred acceptance algorithms: History, theory, practice, and open questions. *international Journal of game Theory* 36 (2008), 537–569.
- [30] Xiaofei Shi and Yanghua Xiao. 2019. Modeling multi-mapping relations for precise cross-lingual entity alignment. In *Proceedings of the 2019 Conference on Empirical Methods in Natural Language Processing and the 9th International Joint Conference on Natural Language Processing (EMNLP-IJCNLP)*. 813–822.
- [31] Zequn Sun, Wei Hu, and Chengkai Li. 2017. Cross-lingual entity alignment via joint attribute-preserving embedding. In *The Semantic Web–ISWC 2017: 16th International Semantic Web Conference, Vienna, Austria, October 21–25, 2017, Proceedings, Part I* 16. Springer, 628–644.
- [32] Zequn Sun, Wei Hu, Chengming Wang, Yuxin Wang, and Yuzhong Qu. 2022. Revisiting embedding-based entity alignment: a robust and adaptive method. *IEEE Transactions on Knowledge and Data Engineering* (2022).
- [33] Zequn Sun, Wei Hu, Qingheng Zhang, and Yuzhong Qu. 2018. Bootstrapping entity alignment with knowledge graph embedding. In *IJCAI*, Vol. 18.
- [34] Zequn Sun, Jiacheng Huang, Wei Hu, Muhao Chen, Lingbing Guo, and Yuzhong Qu. 2019. Transedge: Translating relation-contextualized embeddings for knowledge graphs. In *The Semantic Web–ISWC 2019: 18th International Semantic Web Conference, Auckland, New Zealand, October 26–30, 2019, Proceedings, Part I* 18. Springer, 612–629.
- [35] Zequn Sun, Chengming Wang, Wei Hu, Muhao Chen, Jian Dai, Wei Zhang, and Yuzhong Qu. 2020. Knowledge graph alignment network with gated multi-hop neighborhood aggregation. In *Proceedings of the AAAI conference on artificial intelligence*, Vol. 34. 222–229.
- [36] Zequn Sun, Qingheng Zhang, Wei Hu, Chengming Wang, Muhao Chen, Farahnaz Akrami, and Chengkai Li. 2020. A benchmarking study of embedding-based entity alignment for knowledge graphs. *Proceedings of the VLDB Endowment* 13, 12 (2020).
- [37] Bayu Distiawan Trisedya, Jianzhong Qi, and Rui Zhang. 2019. Entity alignment between knowledge graphs using attribute embeddings. In *Proceedings of the AAAI conference on artificial intelligence*, Vol. 33. 297–304.
- [38] Jihu Wang, Yuliang Shi, Han Yu, Xinjun Wang, Zhongmin Yan, and Fanyu Kong. 2023. Mixed-Curvature Manifolds Interaction Learning for Knowledge Graph-aware Recommendation. In *Proceedings of the 46th International ACM SIGIR Conference on Research and Development in Information Retrieval*. 372–382.

- [39] Zhichun Wang, Qingsong Lv, Xiaohan Lan, and Yu Zhang. 2018. Cross-lingual knowledge graph alignment via graph convolutional networks. In *Proceedings of the 2018 conference on empirical methods in natural language processing*. 349–357.
- [40] Zhichun Wang, Jinjian Yang, and Xiaoju Ye. 2020. Knowledge graph alignment with entity-pair embedding. In *Proceedings of the 2020 Conference on Empirical Methods in Natural Language Processing (EMNLP)*. 1672–1680.
- [41] Y Wu, X Liu, Y Feng, Z Wang, R Yan, and D Zhao. 2019. Relation-Aware Entity Alignment for Heterogeneous Knowledge Graphs. In *Proceedings of the Twenty-Eighth International Joint Conference on Artificial Intelligence*. International Joint Conferences on Artificial Intelligence.
- [42] Y Wu, X Liu, Y Feng, Z Wang, and D Zhao. 2019. Jointly Learning Entity and Relation Representations for Entity Alignment. In *Proceedings of the 2019 Conference on Empirical Methods in Natural Language Processing and the 9th International Joint Conference on Natural Language Processing (EMNLP-IJCNLP)*. Association for Computational Linguistics, 240–249.
- [43] Chengjin Xu, Fenglong Su, and Jens Lehmann. 2021. Time-aware Graph Neural Network for Entity Alignment between Temporal Knowledge Graphs. In *Proceedings of the 2021 Conference on Empirical Methods in Natural Language Processing*. 8999–9010.
- [44] Chengjin Xu, Fenglong Su, Bo Xiong, and Jens Lehmann. 2022. Time-aware entity alignment using temporal relational attention. In *Proceedings of the ACM Web Conference 2022*. 788–797.
- [45] Kun Xu, Linfeng Song, Yansong Feng, Yan Song, and Dong Yu. 2020. Coordinated reasoning for cross-lingual knowledge graph alignment. In *Proceedings of the AAAI conference on artificial intelligence*, Vol. 34. 9354–9361.
- [46] Kun Xu, Liwei Wang, Mo Yu, Yansong Feng, Yan Song, Zhiguo Wang, and Dong Yu. 2019. Cross-lingual Knowledge Graph Alignment via Graph Matching Neural Network. In *Proceedings of the 57th Annual Meeting of the Association for Computational Linguistics*. 3156–3161.
- [47] Rui Ye, Xin Li, Yujie Fang, Hongyu Zang, and Mingzhong Wang. 2019. A vectorized relational graph convolutional network for multi-relational network alignment.. In *IJCAI*. 4135–4141.
- [48] Donghan Yu and Yiming Yang. 2023. Retrieval-Enhanced Generative Model for Large-Scale Knowledge Graph Completion. In *Proceedings of the 46th International ACM SIGIR Conference on Research and Development in Information Retrieval*. 2334–2338.
- [49] Donghan Yu, Yiming Yang, Ruohong Zhang, and Yuexin Wu. 2020. Generalized multi-relational graph convolution network. *arXiv* (2020), 07331.
- [50] Kaisheng Zeng, Chengjiang Li, Lei Hou, Juanzi Li, and Ling Feng. 2021. A comprehensive survey of entity alignment for knowledge graphs. *AI Open* 2 (2021), 1–13.
- [51] Weixin Zeng, Xiang Zhao, Jiuyang Tang, and Changjun Fan. 2021. Reinforced active entity alignment. In *Proceedings of the 30th ACM International Conference on Information & Knowledge Management*. 2477–2486.
- [52] Weixin Zeng, Xiang Zhao, Wei Wang, Jiuyang Tang, and Zhen Tan. 2020. Degree-aware alignment for entities in tail. In *Proceedings of the 43rd International ACM SIGIR Conference on Research and Development in Information Retrieval*. 811–820.
- [53] Qi Zhu, Hao Wei, Bunyamin Sisman, Da Zheng, Christos Faloutsos, Xin Luna Dong, and Jiawei Han. 2020. Collective multi-type entity alignment between knowledge graphs. In *Proceedings of The Web Conference 2020*. 2241–2252.
- [54] Renbo Zhu, Meng Ma, and Ping Wang. 2021. RAGA: relation-aware graph attention networks for global entity alignment. In *Pacific-Asia Conference on Knowledge Discovery and Data Mining*. Springer, 501–513.

Received 20 February 2007; revised 12 March 2009; accepted 5 June 2009